Effects of a Nd—Fe—B Magnetic Filler on the Crystallization of Poly(phenylene sulfide)

PETER C. GUSCHL,[1] HYUN SEOG KIM,[2] JOSHUA U. OTAIGBE[1,2]

[1] Department of Chemical Engineering, Iowa State University, Ames, IA 50011

[2] Department of Material Science & Engineering, Iowa State University, Ames, IA 50011

Received 22 January 2001; accepted 30 May 2001

ABSTRACT: The crystallization of poly(phenylene sulfide) (PPS) in a polymer–magnetic Nd—Fe—B powder suspension was studied. Isothermal crystallization behavior was analyzed by way of differential scanning calorimetry, and the kinetics were described via the Avrami equation. The Avrami parameters and the crystallization times were strongly affected by both the particle size and the presence of a coupling agent coated on the filler particles. The small Nd—Fe—B particles exhibited long induction and half-times, whereas the large particles tended to have short crystallization times. Particles ranging from 38 to 150 μ appeared to have similar crystallization times and to have no significant change in the value of Avrami index with melt crystallization temperature. As a result of these analyses, the dynamic mechanical properties were determined to correlate the fundamental polymer crystallization characteristics and the physical properties of the PPS binder. The enhancement of the wetting of the filler to the binder was promoted through the coupling agent, as confirmed by dynamic mechanical testing performed on the samples. The storage modulus typically decreased because of the presence of the uncoated small particles. Conversely, the loss modulus was enhanced because of the presence of the coated small particles in the PPS binder.
 J Appl Polym Sci 83: 1091–1102, 2002

Key words: polymer crystallinity; magnetic filler; dynamic mechanical property; silane coupling agent; polymer-bonded magnets

INTRODUCTION

Poly(phenylene sulfide) (PPS) is a high-performance engineering thermoplastic that is relatively thermally stable at high temperatures and is resistant to common chemicals and solvents[1,2]. Because of its low impact strength, PPS has been considered inappropriate for applications requiring high-strength materials. However, PPS composites were found to possess a substantial strength[3] when mixed with an inorganic filler, especially in polymer-bonded magnet (PBM) systems such as ours. Because of the semicrystallinity of PPS,[2,3] it is believed that enhanced crystallization of the polymer at the binder–filler interfaces creates reinforcement sites, as others have reported for similar composite systems.[4–6] Thus, it is essential to understand the crystallization behavior of the system for optimal mechanical properties of these composites to be attained.

Because of their advantages, such as low weight in comparison with their purely metallic counterparts, resistance to corrosion, and ease of machining, PBMs have been recognized as a prac-

Correspondence to: J. U. Otaigbe (otaigbe@iastate.edu).

Journal of Applied Polymer Science, Vol. 83, 1091–1102 (2002)

DOI 10.1002/app.10102

tical material for many electromechanical applications, such as automotive (e.g., heating and air conditioning motor, cruise control, door lock, etc.) and nonautomotive (e.g., in computers, spindle drive motors in disk drives, system and modern speaker magnets, etc.). For better thermal stability and enhanced performance of the PBMs, a high-temperature coating, silane-coupling agent is employed, allowing better wetting between the binder and filler as well as adequate oxidative shielding.[7,8] Previous studies have investigated the rheological effects caused by the variation of the particle sizes and by the presence of this coupling agent[9] as well as by other additives such as liquid crystalline polymers introduced into the composite system.[10]

The presence of filler in a semicrystalline polymer can cause many changes to the physical properties of the polymer. Many authors have done extensive work on high-performance thermoplastics such as poly(ether ether ketone) (PEEK)[11] and PPS and their crystallization kinetics both with and without the presence of organic or inorganic fillers.[5,6,12] Caramaro et al.[5] observed a transcrystalline structure (with interphase morphology different from that of the bulk matrix) that formed around carbon fibers suspended in PPS. This observation can help explain the typical increased strength and mechanical properties associated with the addition of filler to a semicrystalline matrix. Some of these typical changes are total degree of crystallinity; crystal phase and its orientation; and number, size, and nature of crystallites.[13] The surface of the filler particles acts as an active site on which the polymer chains can easily adhere, allowing other chains to initiate an ordered crystalline structure around the particle. Various particle sizes and distributions can offer different surface energies that may facilitate crystallization of the polymer chains. The coupling agent promotes a change of interfacial properties of the filler particles, giving rise to better wetting between the filler and polymer binder and ultimately to the increased physical strength of the composite.[13–16] The present study reports the results of an investigation of the effects of particle sizes and a coupling agent on the crystallization behavior of PPS. The study will provide valuable insights into our ability to rationally design useful polymer-bonded magnets with prescribed morphology and properties.

EXPERIMENTAL

Materials

Phillips Chemical Company (Bartlesville, OK) provided the PPS grade—Ryton Type P6. The P6 has been cured at a temperature below its melting point. The average molecular weight value of the P6 is difficult to obtain and estimate because of its synthesis conditions. The density, melting point, and glass transition temperature of the PPS grade are approximately 1.36 g cm^{-3}, 285°C, and 90°C, respectively.

The magnetic powder, manufactured by Magnequench (Anderson, IN), consists of varying particle sizes of a neodymium—iron—boron alloy ($Nd_2Fe_{14}B$) that are produced in platelet form (Fig. 1). Specifically, the commercial powder used is MQP-O, and it has a density of 7.61 g cm^{-3} and a Curie temperature of 299°C, respectively. The particle sizes utilized in these experiments ranged from 38 to 300 μm, separated into five particle size fractions corresponding to the sieve plates used: 38–75, 75–106, 106–150, 150–212, and 212–300 μm. The aspect ratio of the MQP powder was determined to be within the range of 0.2–10.[9]

To prevent oxidation and to promote the coupling (adhesion) effect between the polymer binder and the magnetic powder, 3-aminopropyltriethoxy silane (A1100, Huls) was used as the coupling agent in this study. The MQP-O powders were treated with this coupling agent through simple immersion in an aqueous solution (1 wt % silane). To enhance the wetting of the coupling agent to the powders, we used an ultrasonic homogenizer to blend the powder/silane mixture for a period of 5 min. After the silane treatment, the excess solution was decanted and the powder dried at 80°C in a vacuum oven (Napco, Tualatin, OR) (Model 5861). This method was found to produce the coupled MQP-O powders with reproducible results.

The desired amounts of the coupled powder were hand mixed with the PPS in a plastic bag before additional mixing in a Haake Rheomix 600 (Madison, WI). Rectangular plates (60 $\times$ 60 $\times$ 1.2 mm) were compression molded under a pressure of 7 MPa at 290°C, held for 10 min, and allowed to cool in air to ambient temperature under the same pressure. Thin rectangular bars (18 $\times$ 1.5 $\times$ 1 mm) were machined from the molded plates and used for the dynamical mechanical measurements, whereas small pieces were taken for the crystallization kinetic study.

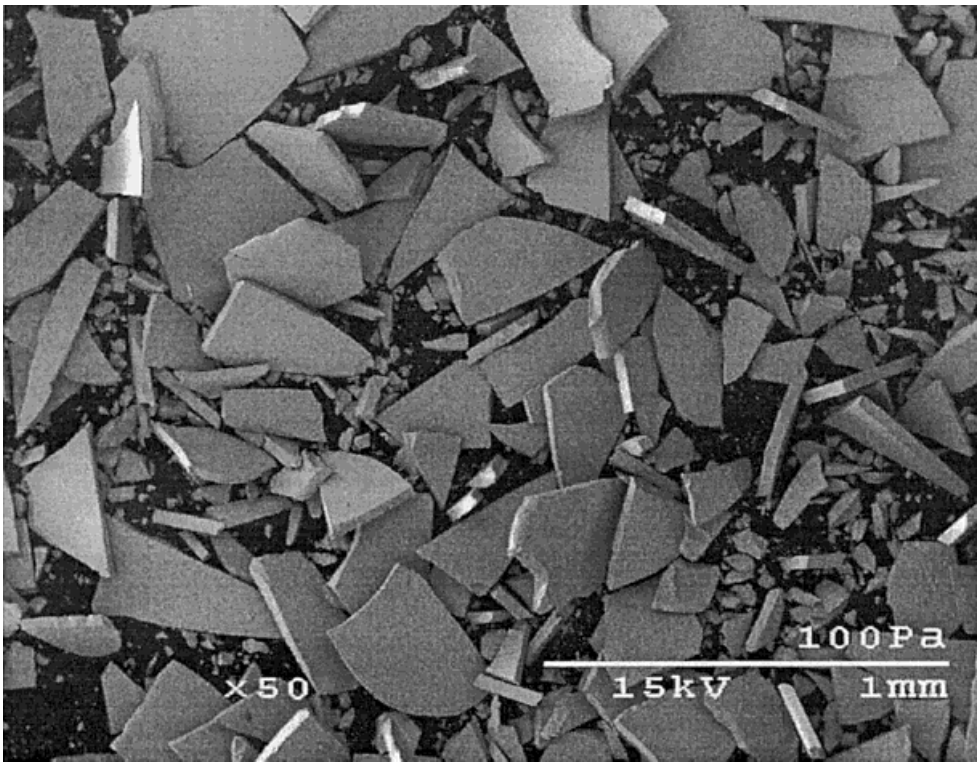

Figure 1 Scanning electron micrograph of typical unsieved MQP-O powder (magnification 50×).

Differential Scanning Calorimetry (DSC)

A differential scanning calorimeter (DSC Pyris 1, Perkin-Elmer thermal analysis system, Boston, MA) was used to determine the crystallization behavior of our samples. The samples were cooled rapidly from above the melting point of PPS to a particular melt crystallization temperature, and the degree of crystallinity was then measured under isothermal conditions. Scanning an indium metal standard at 10°C min^{-1} was used to check the accuracy of the experiments. For the isothermal kinetics study, 10.0 ± 1.0–mg samples were crimped in an aluminum pan and heated from ambient temperature to 320°C at a rate of 10°C min^{-1} in a nitrogen atmosphere. The samples were held at this temperature for 10 min to ensure a total melting of the crystals within the polymer. Four crystallization temperatures, 245, 250, 255, and 260°C, were selected for the isothermal kinetic runs, and the samples were quenched at a rate of 10°C min^{-1} to each isothermal temperature from the holding temperature.

Dynamic Mechanical Analysis (DMA)

Rectangular DMA test specimens (18 × 1.5 × 1 mm) were cut from the compression-molded samples using a slow-speed cutter. A dynamic mechanical analyzer (Perkin-Elmer DMA 7, Boston, MA) was used to perform the testing in a three-point bend configuration, using a specimen span length of 15 mm. Storage (E') and loss (E'') moduli were measured at a frequency of 1 Hz. Temperatures were scanned for each sample at a rate of 2°C min^{-1} from 50 to 220°C. E' linearity was maintained at stress levels producing a displacement amplitude of 30 μ. Confirmation of this linearity was performed through stress scan experiments run at a constant rate of 2 mN min^{-1}, a frequency of 1 Hz, and a temperature of 25°C. Linearity was assumed to hold for different values determined at the higher temperatures tested.

Microscopy

Both coated and uncoated PBM samples were mounted into a two-part epoxy matrix from Buehler (resin: number 20-8128-032; hardener: number 20-8128-008). After curing the epoxy and allowing it to set, the samples were polished on metallographic wheels with increasingly fine abrasives to produce a smooth surface for environmental scanning electron microscopy and optical microscopy examination.

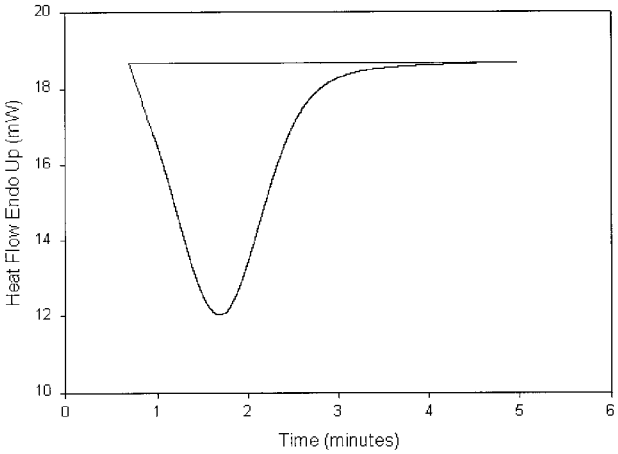

Figure 2 Endothermic isothermal thermogram of neat poly(phenylene sulfide) cooled from 320 to 245°C.

RESULTS AND DISCUSSION

Isothermal Crystallization Behavior

To describe the kinetics of the crystallization behavior, the Avrami equation, also known as the "stretched exponential" equation, was employed, revealing the correct relationship between the degree of crystallization, X, and time, t.[17]

$$X(t, T) = 1 - \exp[-(kt)^n] \tag{1}$$

The k and n parameters are constants, where k (units of s^{-1}) contains several material constants and is defined as the propagation rate constant of the crystal, and n (dimensionless) is a number that depends on the geometry of the growth process. X is defined as the time- and temperature-dependent ratio of the crystallized mass to the original amorphous polymer mass. Avrami has treated intermediate heterogeneous nucleation cases in which the rate of nucleation decreases exponentially with time.[3]

For the isothermal kinetics studies, pure PPS was tested in the temperature range of 230–265°C. It was noticed that in experiments performed at temperatures below 240°C crystallization was too fast to measure accurately, and that in those performed at temperatures above 265°C the crystallization was too slow. However, stable thermograms were obtained for the following temperatures: 245, 250, 255, and 260°C. The thermogram data (see Fig. 2 for a typical thermogram) reveal that the time needed for the crystallization peak to develop is a strong function of temperature, such that at higher temperatures, more crystallization time is required. Analysis of the relative crystallinity at each temperature was performed through the division of the area of the crystallization peak at various times by the value of the total heat of crystallization over the entire thermogram area, represented by the following equation:[10]

$$X_c = \frac{\int_0^t (dH/dt)dt}{\int_0^\infty (dH/dt)dt} \tag{2}$$

As Equation (2) yields a mass fraction of crystallinity, one must convert to volume fraction for consistency in the use of Equation (1):

$$X_{vc} = \frac{X_{mc}\rho_a}{\rho_c - X_{mc}(\rho_c - \rho_a)} \tag{3}$$

ρ_a and ρ_c represent the amorphous and crystalline densities, respectively, and the subscripts vc and mc are the volume and mass fractions of crystallinity, respectively. The density values and equation were obtained from Kenny et al.[18] The analysis of these data for relative crystallinity is rep-

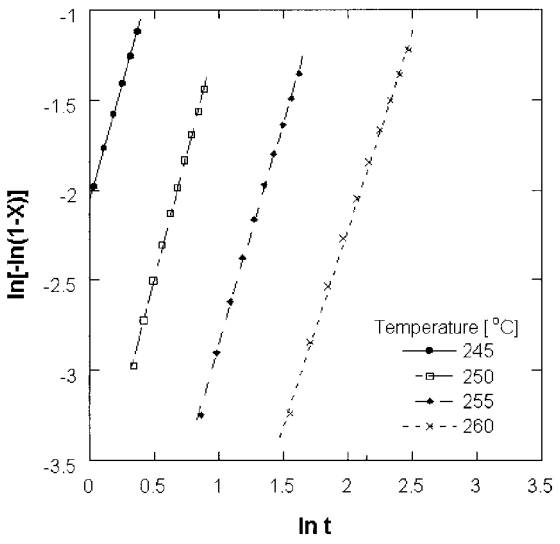

Figure 3 Linearized Avrami equation graph of neat poly(phenylene sulfide) at the melt crystallization temperatures 245, 250, 255, and 260°C.

resented in Figure 3. Through application of the Avrami equation on the partially integrated heat flow changes during isothermal crystallization, the parameters k and n could be determined. Rearrangement of Equation (1) by applying a double logarithm to both sides of the equation yields a linear form with variables $\ln[-\ln(1-X)]$ and $\ln t$ and slope n and intercept $n \ln k$. From these results, the parameters appear to be functions of crystallization temperature as observed in earlier PPS crystallization studies reported elsewhere.[5,6,12] The index n increases for the neat PPS samples and decreases weakly with temperature, but it appears to reduce as the coupling agent is employed [see Fig. 4(a)]. Caramaro et al.[5]

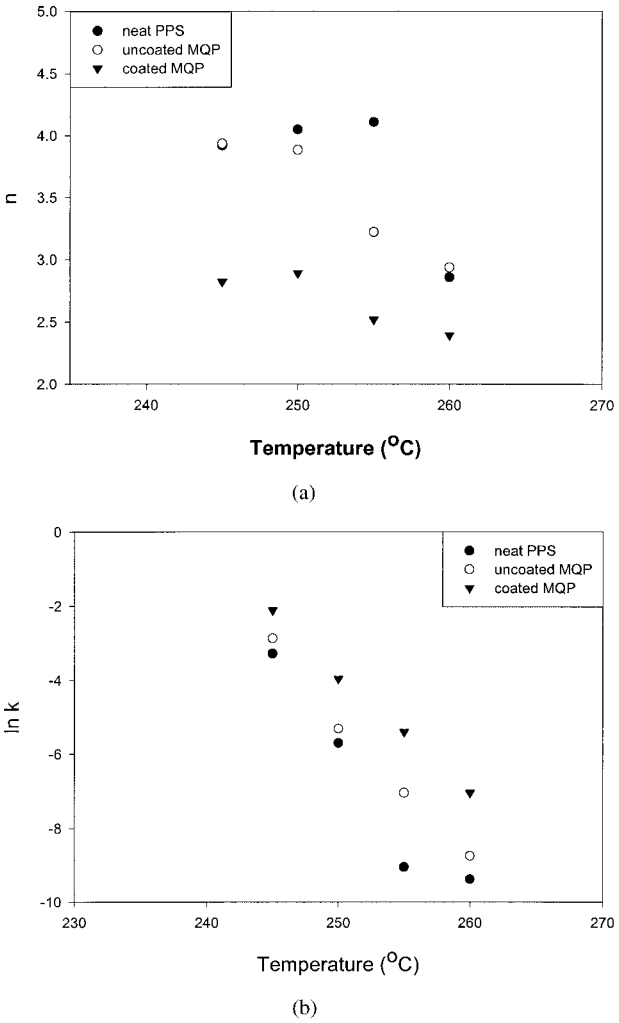

Figure 4 Effect of filler and coupling agent on the Avrami parameters (a) n and (b) k of a 15 vol% MQP suspension at the four isothermal crystallization temperatures.

Table I Avrami Index for Isothermal Polymer Crystallization and Interpretation[19]

n	Nucleation	Growth Geometry	Growth Control
2	Instantaneous	Disc	Interface
2	Homogeneous	Disc	Diffusion
2	Homogeneous	Rod	Interface
2.5	Homogeneous	Sphere	Diffusion
3	Instantaneous	Sphere	Interface
3	Homogeneous	Disc	Interface
4	Homogeneous	Sphere	Interface

reported similar results for the Avrami index, n, and melt crystallization temperature. The rate constant k decreases significantly as the temperature increases, as shown in Fig. 4(b). The kinetic parameters obtained in this study are also consistent with those reported by Brostow et al.[12] and Minkova et al.,[19] who performed their melt crystallization studies on PPS in the ranges of 225–235°C and 200–240°C. The neat PPS and uncoated composite of MQP-O/PPS showed indices between 4.0 and 2.5 as the temperature was increased. The coated composite, however, exhibited the smaller range of indices of 2.5–2.0. These results indicate that the crystal growth mechanism and nucleation type changed because of the addition of the coupling agent (see Table I).[20] A summary of these parameter values is shown in Table II for the neat PPS, uncoated MQP–PS composite, and coated MQP–PPS composite.

Once information regarding the k and n parameters was known, the half-time of the crystal growth was determined. This half-time is the time required to obtain a relative crystallinity of 50% ($X = 0.5$). Applying this value to Equation (1) gives the following equation:

$$t_{1/2} = \frac{(\ln 2)^{1/n}}{k} \tag{4}$$

Figure 5 represents the temperature dependence of the crystallization rates of the neat PPS and the uncoated and coated MQP-O/PPS composite systems. The presence of the powder and coupling agent seems to accelerate the crystallization of the PPS polymer, especially when they are present at lower melt crystallization temperatures. This observation can be explained as an adhesion effect of the coupling agent to the filler

Table II Avrami Parameters and Half Times of Crystallization for Neat, Uncoated, and Coated MQP Particles in PPS

Melt Crystallization Temperature (°C)	Neat PPS			Uncoated MQP			Coated MQP		
	n	k (s^{-1})	$t_{1/2}$ (min)	n	k (s^{-1})	$t_{1/2}$ (min)	n	k (s^{-1})	$t_{1/2}$ (min)
245	3.92	0.433	2.10	3.94	0.482	1.89	2.82	0.473	1.86
250	4.05	0.245	3.73	3.89	0.255	3.57	2.89	0.254	3.47
255	4.11	0.111	8.26	3.22	0.113	7.93	2.52	0.117	7.37
260	2.86	0.038	23.40	2.94	0.051	17.31	2.39	0.053	16.26

PPS, poly(phenylene sulfide)

particles[9] that provides nucleation enhancements of the semicrystalline binder.[17] The enhancement of nucleation can be attributed to an increase in the number of active nucleation sites on the surface of the filler particles.

Good agreement of the pure PPS calculations of half-time of crystallization between Lopez and Wilkes[21] and Jog and Nadkarni[22] is observed (see Fig. 6). Although the agreement with the aforementioned authors' work is quite reasonable, discrepancies arose with the results of Desio and Rebenfeld[6] and Minkova et al.[19] The general trend of crystallization temperature is apparent, as is the position of the $t_{1/2}$ minimum in the temperature range of 160–170°C, which can be extrapolated from the work of Minkova et al.[19] The differences in results can be attributed to dissimilar molecular weights of the PPS studied, as well as to thermal history effects on the PPS. For example, our samples were prepared in a batch mixer under previously mentioned thermal and shear conditions before the crystallization measurements were taken, which may have affected the crystalline properties of the polymer.

The effect of particle size on the crystallization behavior was also investigated. Figures 7 and 8 show the crystallization temperature dependencies of the index and the half-time for the different particle sizes, respectively. It appears that the monodispersed composite of average particle size 128 μ (106–150-μ range) yielded the lowest index range that did not change much with temperature. The mixture of particles of each size (polydispersed, unsieved MQP) showed the largest drop in index value from about 3.3 to 2.4. The size of the particles is an important factor in reference to the surface energy of the particles. As particle size changes, the interaction behavior of the com-

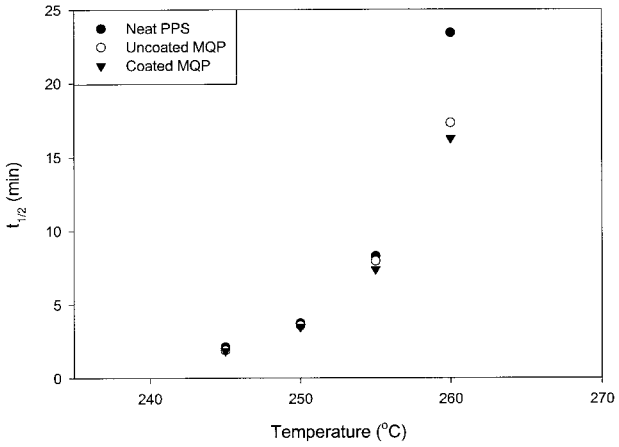

Figure 5 Effect of filler and coupling agent on half-time crystallization for a 15 vol% MQP suspension at the four isothermal crystallization temperatures.

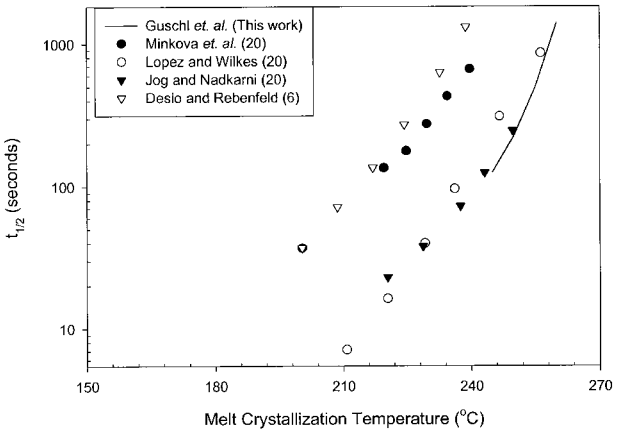

Figure 6 Half-time of crystallization of pure poly(phenylene sulfide) versus melt crystallization temperature.

ponents of the composite (the filler and polymer) is altered.[23] Figure 8 shows that particle size affects the half-time of crystallization. The small MQP particles have long half-times of crystallization, whereas the large particles exhibit short half-times (see Table III).

Calculation of the crystallization induction time was graphically determined through a linear extrapolation method, as direct calculation was not possible through use of the Avrami equation. Linear extrapolation allows one to evaluate a steady-state induction time for nucleation of crystals effectively and consistently.[24,25] Figure 9 represents a graph of relative crystallinity versus crystallization time. The induction time of crystallization can be found by determining the line tangent to the curve during the rise in relative crystallinity. Extrapolating back to the initial relative crystallinity value allows one to evaluate the induction time. Figure 10 reveals the trend of induction time with crystallization temperature and how it is affected by the presence of the filler particles and coupling agent. Apparently, the MQP powder causes a short induction period in which the polymer crystals can grow. The coupling agent reduces this induction time further. Similar trends were observed regarding the half-time versus temperature data in Figure 5. However, the induction times appeared to be more sensitive to the presence of the filler and the coupling agent. A correlation between the half-time of crystallization and the induction time for crystal growth can be drawn. As the presence of the MQP filler particles and the coupling agent induces a quicker crystallization than if no particles were present, one can say that the half-time would also be shortened under a similar mechanism. Also, the rise in induction time with temperature was not as drastic as that for the samples containing the filler and the coupling agent. In regard to particle size, the temperature dependence of the induction time (shown in Fig. 11) behaved similarly to that of the half-time (Fig. 8). Larger particles, specifically those in the 106–150-μ range, induce a quicker crystallization in terms of both half-times and induction times. Furthermore, the unimodal systems of finer particles (i.e., <38 μ) tended to have slower induction times than those of the large particles.

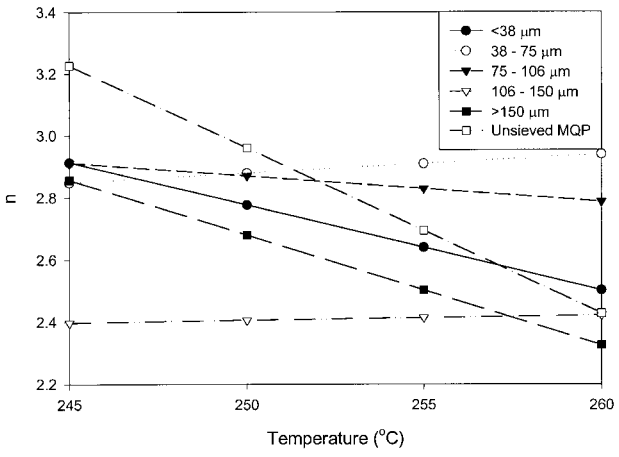

Figure 7 Effect of particle size (for uncoated MQP) on the index of a 15 vol% MQP suspension at the four isothermal crystallization temperatures.

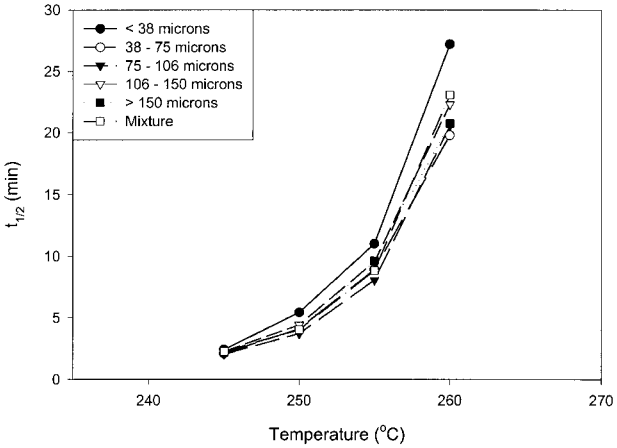

Figure 8 Effect of particle size (for uncoated MQP) on the calculated half-time crystallization of a 15 vol% MQP suspension at the four isothermal crystallization temperatures.

Dynamic Mechanical Analysis

The mechanical properties of the filled polymeric composite were investigated, and the results showed a significant improvement in the storage (elastic component) and loss (viscous component) moduli, caused by the presence of the coupling agent (Figs. 12 and 13). The filler induced an increase of roughly 33% in the storage modulus of the neat PPS, whereas the coupling agent gave an increase of about 56%. The loss modulus data show an increase when filler and the coupling agent are added to the PPS binder, emphasizing an enhanced mechanical damping character of the composite. Because the presence of the filler and coupling agent strengthens the polymer (increasing storage modulus) and creates

Table III Avrami Index and Half Times of Crystallization of PPS Containing Uncoated MQP Particles, With the Sizes Shown

Melt Crystallization Temperature (°C)	<38 Microns		38–75 Microns		75–106 Microns	
	n	$t_{1/2}$ (min)	n	$t_{1/2}$ (min)	n	$t_{1/2}$ (min)
245	3.05	2.42	2.93	2.10	2.93	2.03
250	2.55	5.43	2.80	4.10	2.84	3.71
255	2.67	11.01	2.80	8.91	2.83	8.05
260	2.56	27.19	3.04	19.79	2.80	20.57
	106–150 Microns		>150 Microns		Mixture	
	n	$t_{1/2}$ (min)	n	$t_{1/2}$ (min)	n	$t_{1/2}$ (min)
245	2.43	2.26	2.87	2.18	3.30	2.26
250	2.39	4.42	2.65	4.03	2.83	4.03
255	2.36	9.53	2.54	9.61	2.77	8.83
260	2.46	22.29	2.32	20.73	2.43	23.07

PPS, poly(phenylene sulfide).

a material with high damping characteristics (increasing loss modulus), a change in *tan* δ was observed. Furthermore, Figure 13 reveals a shifted glass transition temperature (indicated by the arrow) as filler and coupling agent are added to the polymer matrix. The T_g (glass-transition temperature [°C]) is increased slightly because of the presence of these additives, which suggests an improvement on the thermal stability of the PPS binder. The reasons for these observations can be attributed to the effects of adhesion and nucleation enhancement between the filler and binder, as mentioned previously.[20,23,26] Figure 14 represents the effect of three different particle sizes on the storage modulus and *tan* δ (ratio of loss to storage modulus). Essentially, the large MQP particles (>150 μ) showed the highest storage modulus and lowest *tan* δ values, compared

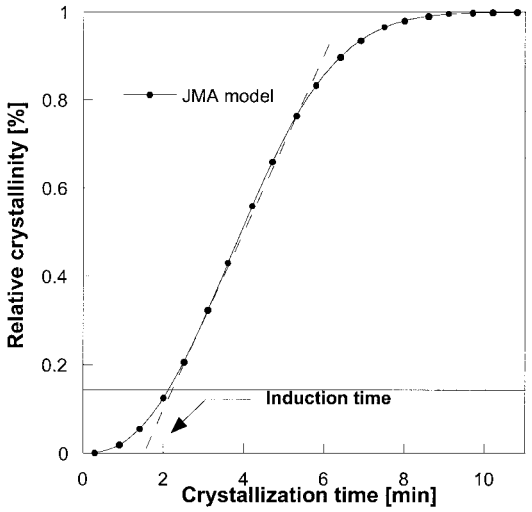

Figure 9 Schematic for determination of induction time of crystallization.

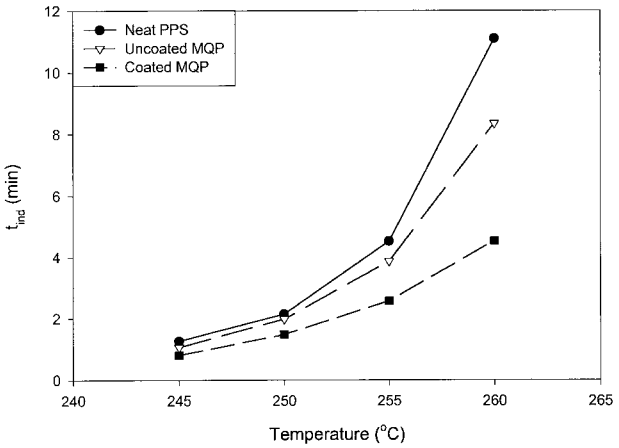

Figure 10 Effect of filler and coupling agent on the estimated induction time of crystallization for a 15 vol% MQP suspension at the four isothermal crystallization temperatures.

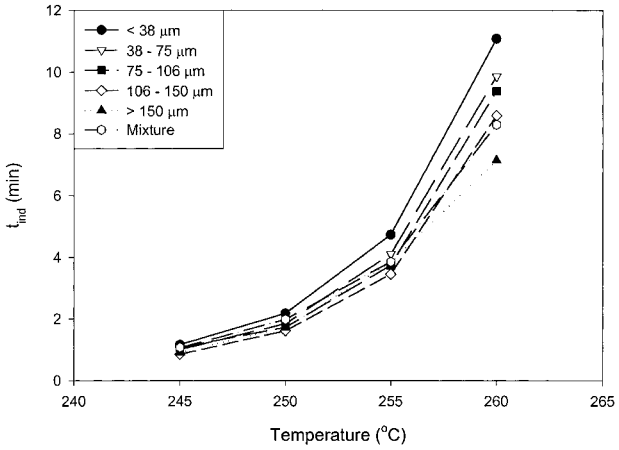

Figure 11 Effect of particle size (for uncoated MQP) on the estimated induction time of crystallization for a 15 vol% MQP suspension at the four isothermal crystallization temperatures.

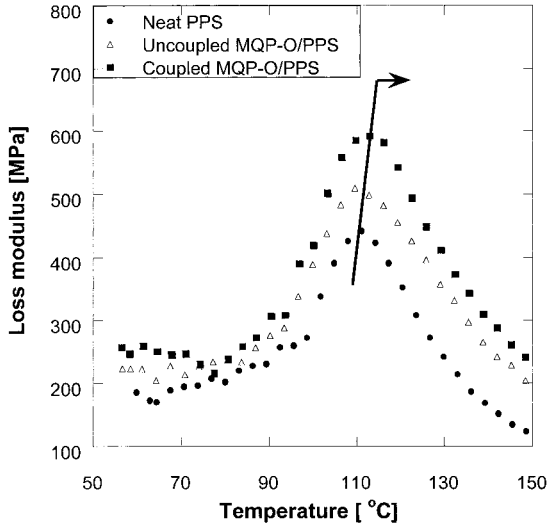

Figure 13 Effect of the presence of filler and coupling agent on the loss modulus of the suspensions of 15 vol% MQP in the temperature range of 50–150°C.

with those of the smaller particulate PBM samples (<38 and 75–106 μ) at temperatures above the glass transition. The small particles possess a high degree of attraction for each other and for neighboring particles. These particle–particle interactions result in increasing resistance to flow, inducing a large dampening characteristic in the composite. The large particles do not interact as strongly as the small particles, and, because of their size and ability to disperse more regularly than the small particles, they tend to reinforce the PBM.

Figure 15(a,b) consists of optical micrographs of the composite material with both uncoated and coated particles, respectively. These pictures show, to some extent, the crystalline enhancement caused by the presence of the MQP filler and the coupling agent on the semicrystalline PPS matrix. One can see a structure (dark spots) present along the surface between the particle and matrix in both micrographs that is not evident within the bulk of the matrix, where

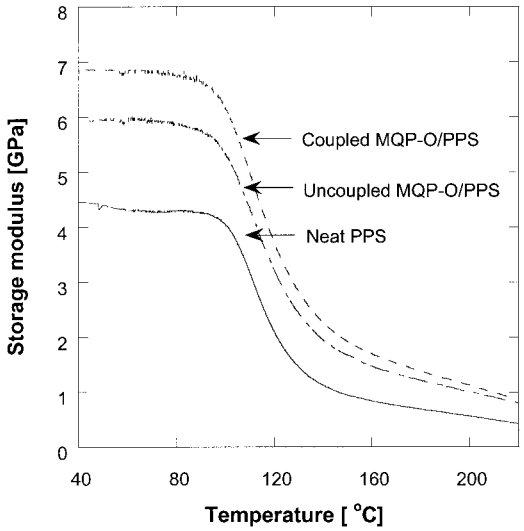

Figure 12 Effect of the presence of filler and coupling agent on the storage modulus of the suspension in the temperature range of 40–220°C.

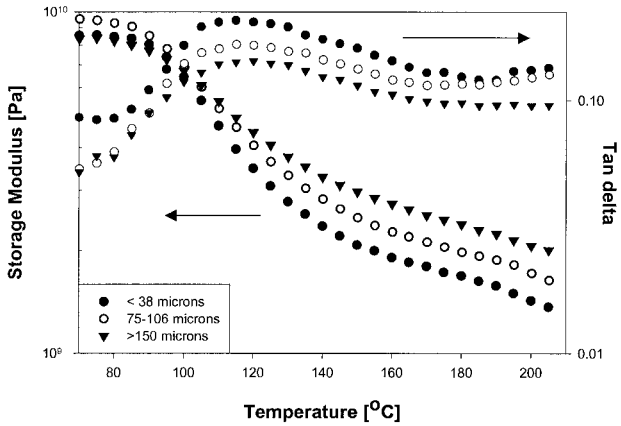

Figure 14 Effects of particle size on the storage modulus and phase angle shift of the suspensions of 15 vol% MQP (uncoated) in the temperature range of 60–220°C.

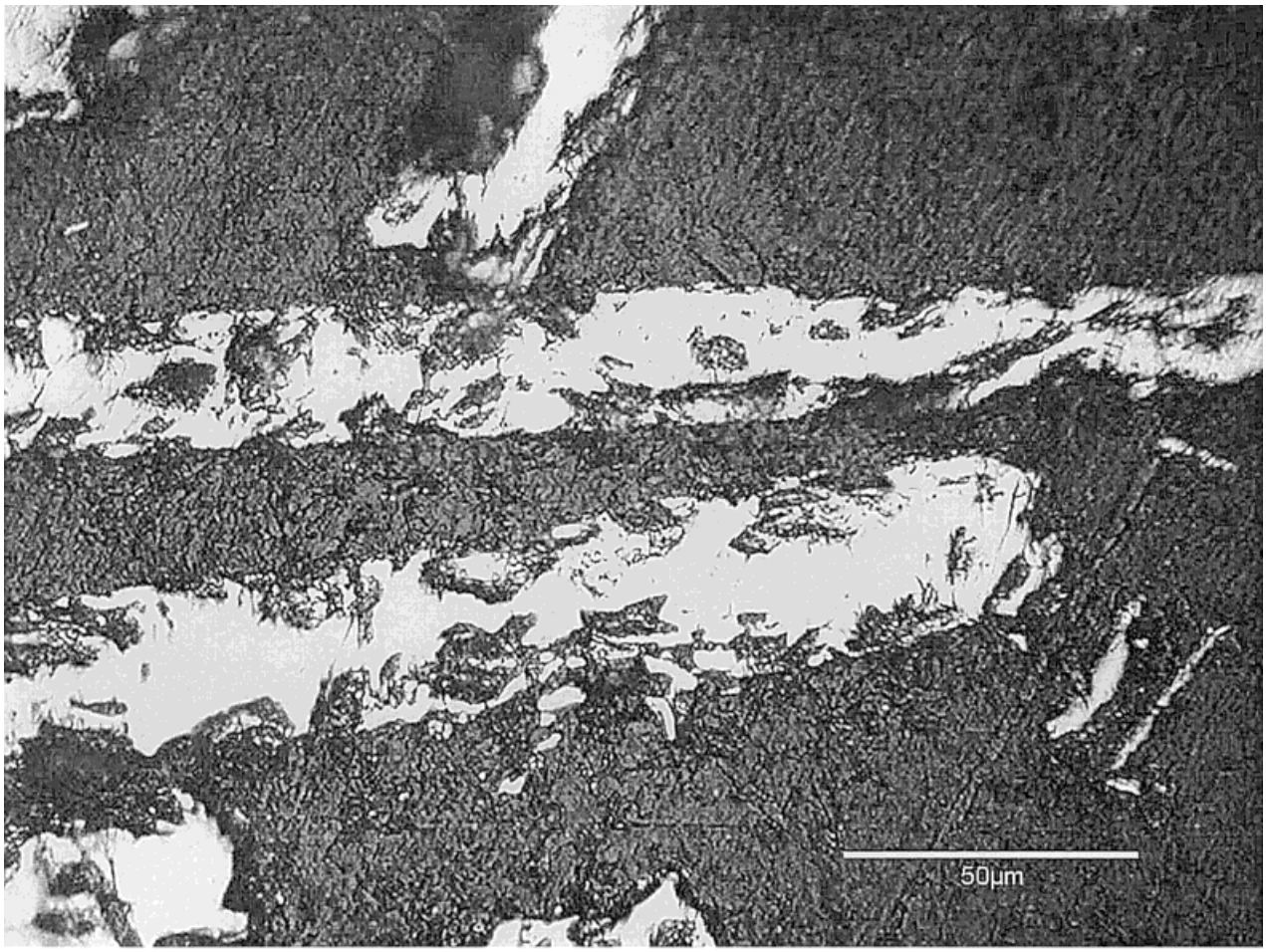

(a)

Figure 15 Optical micrographs of (a) uncoated and (b) coated MQP particles in poly(phenylene sulfide).

no particles exist. It is apparent that more of these dark spots are visible around the coated particles in Figure 15(b). Small particles appear to be more homogeneously surrounded by this crystalline structure than do the large particles. This observation supports the fact that the presence of small particles in the matrix gives rise to a composite with a higher mechanical damping character (*tan* δ). If the local crystallinity were higher for the small particles than for the large particles, then interactions between the small particles would be stronger because of the ordered structure surrounding them, thus impeding the polymer flow around these obstacles during DMA testing. Additional microscopic evidence for the effects of the MQP filler on the dynamic mechanical behavior of the PBM is reported elsewhere.[9,16]

CONCLUSIONS

This study shows that the crystallization behavior of a semicrystalline polymer binder, PPS, was significantly changed by the presence of Nd—Fe—B inorganic filler (MQP-O) and a silane-coupling agent. It was observed that the MQP-O powder acted as a nucleation agent, initiating faster crystallization by reducing the half-time and induction time of crystallization. Particle size did not appear to affect the crystallinity of the composite significantly, but small particles did exhibit the longest crystallization times. The Avrami index, n, is at a minimum for the 106–150-μ particle size range and did not vary strongly with crystallization temperature. Large particles and coated particles (>150 μ) seemed to have the highest storage modulus and the lowest

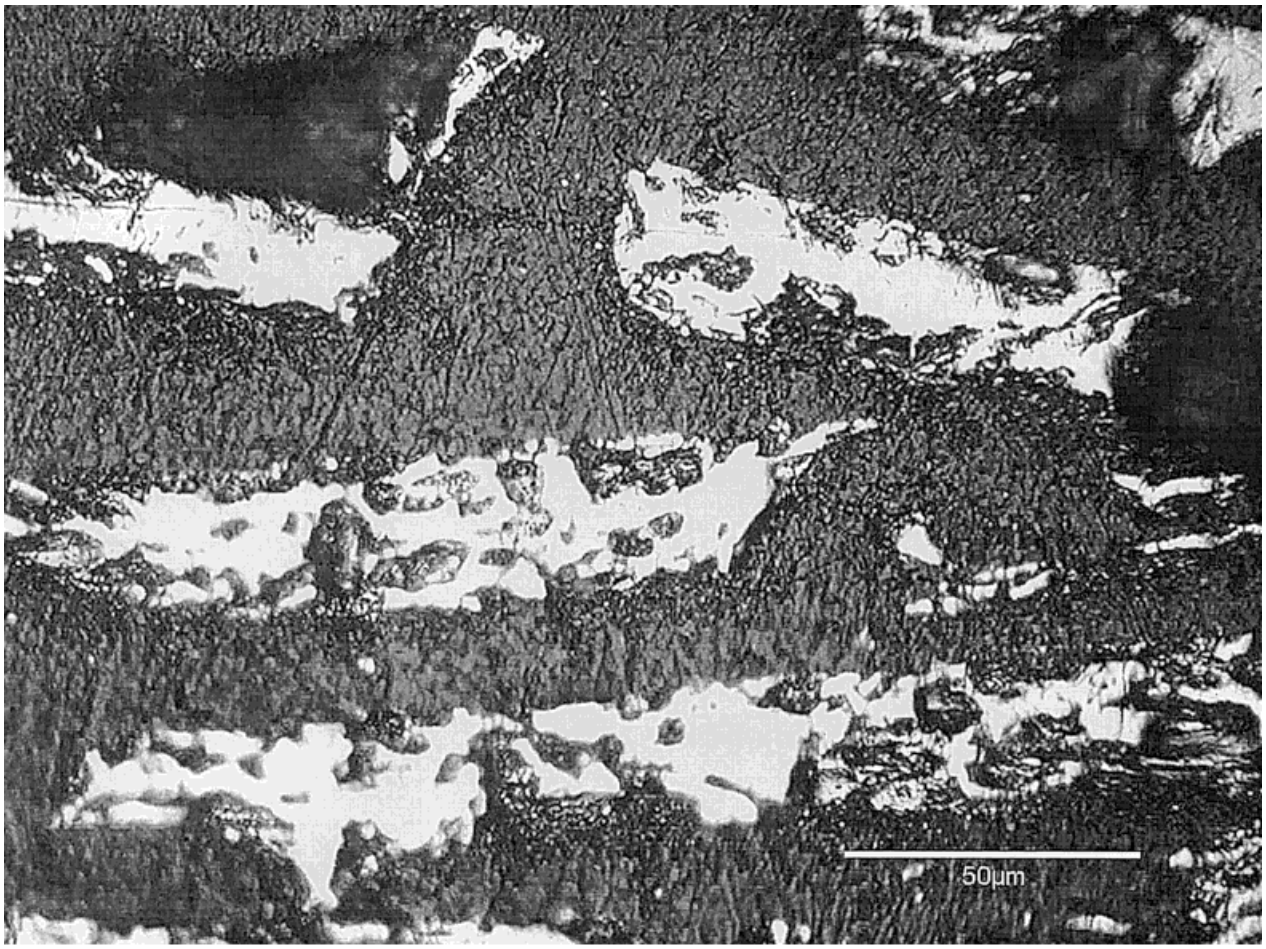

(b)

Figure 15 (*Continued from the previous page*)

mechanical damping, *tan* δ, for temperatures above the glass transition temperature. The presence of the particles in a mixture of different sizes did not appear to affect the crystallization behavior significantly; however, the largest change in the index *n* was observed for this particle configuration. The coupling agent further enhances this crystallization via improved wetting between the particle and polymer chains. The net effect of this faster growth causes an internal strengthening to occur within the composite, giving rise to an improvement in mechanical properties.

The financial support from the U.S. National Science Foundation through grant DMR-9712688 is highly appreciated. We are particularly grateful to Group Arnold and Mr. Steve Constantinides, without whose collaboration this work would have been impossible. The anonymous reviewer is also thanked for the critical comments that improved the quality of this manuscript.

REFERENCES

1. Hill, H.; Brady, D. G. Polym Eng Sci 1976, 16, 831.
2. Brady, D. G. J Appl Polym Sci 1976, 20, 2541.
3. Kenny, J. M.; Maffezzoli, A. Polym Eng Sci 1991, 31, 607.
4. Song, S. S.; White, J. L.; Cakmak, M. Polym Eng Sci 1990, 30, 944.
5. Caramaro, L.; Chabert, B.; Chauchard, J. Polym Eng Sci 1991, 31, 1279.
6. Desio, G. P.; Rebenfeld, L. J Appl Polym Sci 1990, 39, 825.
7. Kowalewski, T.; Galeski, A. J Appl Polym Sci 1986, 32, 2919.

8. Long, Y.; Shanks, R. A.; Stachurski, Z. H. Prog Polym Sci 1995, 20, 651.
9. Otaigbe, J. U.; Kim, H. S.; Xiao, J. Polym Compos 1999, 20, 697.
10. Guschl, P. C.; Otaigbe J. U. Polym Compos, to appear. See also Guschl, P. M.S. Thesis, Iowa State University, 2000.
11. Velisaris, C. N.; Seferis, J. C. Polym Eng Sci 1986, 26, 1574.
12. Brostow, W.; Seo, K.;. Baek, J. B.; Lim, J. C. Polym Eng Sci 1995, 35, 1016.
13. Rothon, R. Particulate-Filled Polymer Composites; Longman Scientific & Technical: Essex, 1995.
14. Han, C. D.; Sandford, C.; Yoo, H. J. Polym Eng Sci 1978, 18, 849.
15. Boaira, M. S.; Chaffey, C. E. Polym Eng Sci 1977, 17, 715.
16. Xiao, J.; Kim, H. S.; Otaigbe, J. U.; Tacke, T. SPE ANTEC Tech Papers 1999, 55, 3936.
17. Maffezzoli, A.; Kenny, J. M.; Torre, L. Thermochim Acta 1995, 269/270, 185.
18. Kenny, J. M.; Maffezzoli, A.; Nicolais, L. Thermochim Acta 1993, 227, 83.
19. Minkova, L.; Paci, M.; Pracella, M.; Magagnini, P. Polym Eng Sci 1992, 32, 57.
20. Schultz, J. Polymer Material Science; Prentice-Hall: Englewood Cliffs, NJ, 1974.
21. Lopez, L. C.; Wilkes, G. L. Polymer 1988, 29, 106.
22. Jog, J. P.; Nadkarni, V. M. J Appl Polym Sci 1985, 30, 997.
23. Denault, J.; Vu-khanh, T. Polym Comp 1992, 13, 372.
24. Wunderlich, B. Macromolecular Physics II. Crystal Nucleation, Growth, Annealing; Academic Press; New York 1976; p 65.
25. Wang, C.; Liu, C. J Polym Sci Part B Polym Phys 1998, 36, 1361.
26. Mitsuishi, K.; Ueno, S.; Kodama, S.; Kawasaki, H. J Appl Polym Sci 1991, 43, 2043.